Seismic Behavior of Precast Columns with High-Strength Steel Coiled Strip Reinforcement

ACI Foundation: Concrete Research Council
Final Report

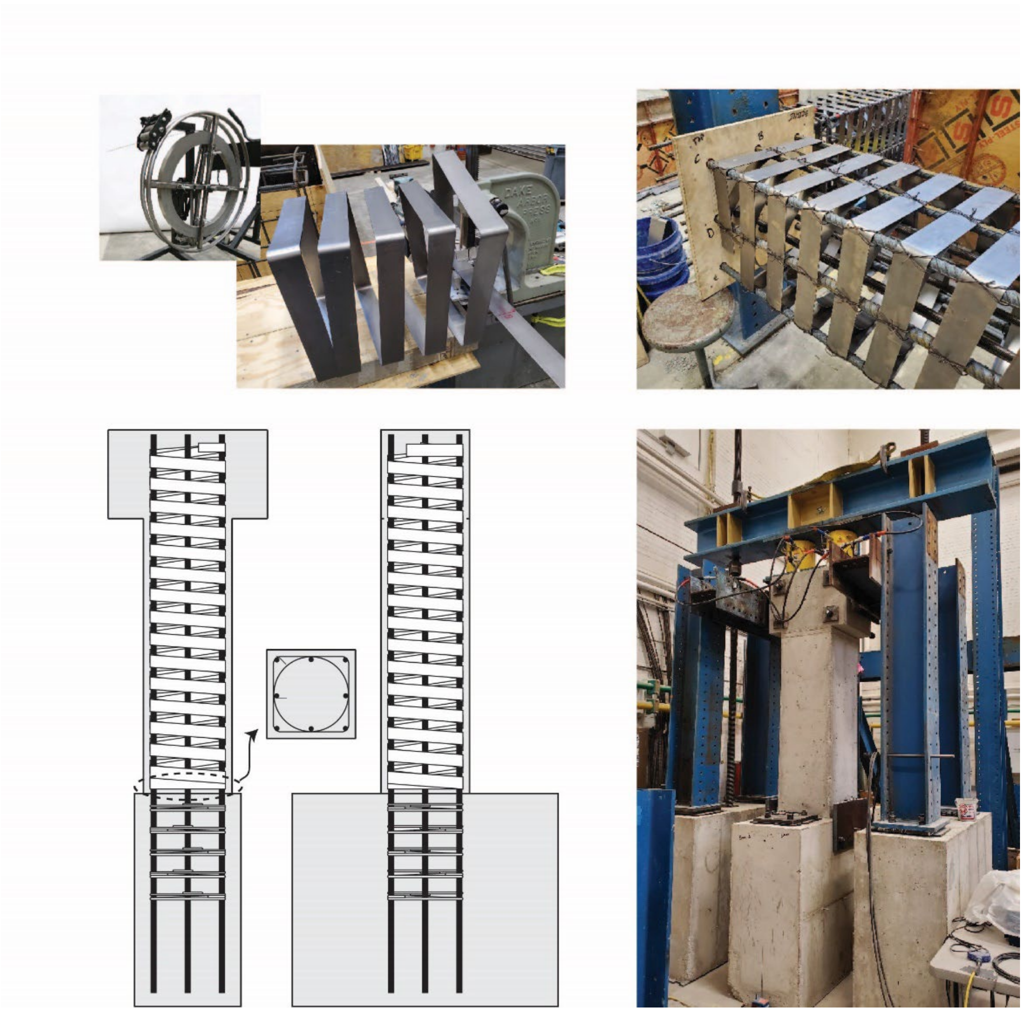

Steven M. Barbachyn
Shane Oh
Lily Polster
Ashley P. Thrall (PI)
Brad D. Weldon
Yahya C. Kurama (Co-PI)

ABSTRACT

This report presents the experimentally investigation of the behavior of square reinforced concrete (RC) columns with high-strength [100 ksi (690 MPa) yield strength] steel coiled strips as embedded confinement reinforcement under reversed-cyclic lateral loading and a constant axial compression load. Six full-scale specimens [20 in. x 20 in. (508 mm x 508 mm) cross-section] were tested with varying: (1) confinement type (strip versus reinforcing bar), (2) confinement layout (hoops/ties, single spiral, two spirals, two spirals out-of-phase), and (3) confinement reinforcement ratio. Findings include: (1) the strip-confined specimens had a similar peak strength as the rebar-confined specimen and the peak strength exceeded analytical predictions, (2) the initial stiffness of the strip-confined specimens was greater than the rebar-confined specimen, (3) all of the specimens met the ACI T1.1-01 criterion that the lateral load at 3.5% drift was not below 75% of the peak, and (4) strip-confined specimens demonstrated improved residual strength behavior compared to the rebar-confined specimen. Overall, this study demonstrates the promise of strip-confinement for RC columns in seismic regions.

INTRODUCTION

Ductile, high-strength [yield strength of 100 ksi (690 MPa)] coiled steel strips (Figure 1A), in either hoop or spiral configuration, can offer a new approach to embedded confinement for reinforced concrete (RC) structures. Potential advantages of strip confinement, as opposed to conventional deformed reinforcing bar hoops and cross-ties, include increased: (1) volume of confined concrete due to the wider and thinner strip, (2) effective depth as the thinner strip enables closer placement of the extreme longitudinal reinforcing bars to the edge of the member, and (3) restraint against longitudinal bar buckling after concrete cover spalling due to the larger width of the strips. Additional fabrication benefits include: (1) rapid placement as strips can be uncoiled, bent, and tied without splices, and (2) reduced congestion and improved concrete placement as the thin strips can have smaller bend radii. Figure 1B illustrates these potential advantages providing a direct comparison between a conventionally confined column using Grade 100 (Metric Grade 690) reinforcing bar hoops and ties and a strip-confined column using high-strength steel spirals, with an outer square perimeter spiral and an inner circular spiral. Each meets the American Concrete Institute (ACI) *Building Code Requirements for Structural Concrete (ACI 318-19) and Commentary (ACI 318R-19)* (ACI 318-19, hereafter) specifications for columns of special moment frames. Aside from the geometric potential of strip reinforcement, high-strength steel coil, such as the dual-phase (DP) 980/700 [yield strength of 100 ksi (690 MPa)] that was used in this study, can provide increased strength as compared to Grade 60 (Metric Grade 420) deformed reinforcing steel and increased ductility as compared to Grade 100 (Metric Grade 690) deformed reinforcing steel (Figure 2).

Given the potential benefits of this novel type of confinement reinforcement, this research experimentally investigates the lateral behavior of square RC columns with embedded DP 980/700 strip confinement. Specifically, six full-scale specimens [with 20 in. x 20 in. (508 mm x 508 mm) cross-section] were tested under reversed-cyclic lateral loading and a constant applied concentric axial compression load. Varied parameters include: (1) confinement type (strip versus reinforcing bar): (2) confinement layout (hoops/ties, single spiral, two spirals, two spirals out-of-phase); and (3) confinement reinforcement ratio.

Barbachyn et al. (2023) previously experimentally investigated the axial load behavior of square, strip-confined, RC columns. Specifically, reduced-scale column specimens [8 x 8 in. and 10 x 10 in.(203 mm x 203 mm and 254 mm x 254 mm)] were tested under concentric axial compression until failure. Although a control (conventional) specimen confined using deformed reinforcing bar ties exhibited greater post-peak residual strength and better ductility than the strip-confined specimens, key results included: (1) all strip-confined specimens exhibited peak strengths exceeding the nominal axial strength predicted by ACI 318-19, (2) the strip-confined specimens had a similar ratio of peak axial strength to nominal axial strength as well as similar pre-peak stiffness compared to the control specimen, (3) using an outer, square strip spiral and an inner circular strip spiral improved the post-peak residual strength and ductility for a cross-section with eight longitudinal reinforcing bars, and (4) strip spiral or hoops can provide improved constraint to prevent corner bar buckling in comparison to that provided by conventional reinforcing bar hoops. This pilot study demonstrated the viability of the strip confinement and provided valuable data that informed the current study (e.g., indicating the benefits of two strip spirals). However, it only focused on the axial compression behavior of strip-confined columns (i.e., no lateral load was applied). To understand the behavior of strip-confined RC columns for earthquake resistant design, it is necessary to conduct an experimental evaluation under reversed-cyclic lateral loads and a constant applied concentric axial compression load. This is the focus of the current investigation.

Aside from the above-mentioned study by the authors, there has been no research investigating steel strip as embedded confinement reinforcement in the United States, although Robert Cummings used steel strip hoops as reinforcement dating back to 1911 (Kidder and Nolan 1911). Elsewhere, Shafqat and Ali (2012) performed axial compression tests on RC columns confined using steel strips hoops. Also using steel strip hoop confinement, Tahir et al. (2014) performed cyclic axial load tests on RC columns. Rizwan (2009) investigated the behavior of RC columns confined using steel strip hoops in the hinge zone (with conventional reinforcement elsewhere) under reversed-cyclic lateral load and sustained axial load [see also Rizwan et al (2016)]. There is no existing research on the lateral load behavior of RC columns confined by steel strip spirals.

RESEARCH SIGNIFICANCE

This report presents the measured behavior of five square RC columns confined using dual-phase, high-strength steel coiled strips under reversed-cyclic lateral loading combined with constant applied concentric axial compression loading, as compared to the behavior of a conventional control column with high-strength reinforcing bar confinement. This is the first research on the lateral load behavior of strip-confined RC columns in the United States. The experimental results provide new knowledge on a novel approach for confinement reinforcement with the potential to improve the behavior of RC columns subjected to seismic loads and to accelerate fabrication.

EXPERIMENTAL INVESTIGATION

Six full-scale [20 in. x 20 in. (508 mm x 508 mm) cross-section] RC columns were tested under a prescribed lateral loading protocol followed by a prescribed lateral displacement protocol, while also being subjected to a constant concentric axial compression load (Figure 3 and Table *1*). For specimen labels, the first term denotes confinement reinforcement type and layout (RH=reinforcing bar hoops; 2SS=two strip spirals; 2SSO=two strip spirals that are out-of-phase; SST=one strip spiral with cross-ties; see Figure 4) and the second third term denotes volumetric confinement reinforcement ratio as a percentage.

Specimens

The 20 in. x 20 in. (508 mm x 508 mm) specimen cross-section was chosen as it is within the range of typical dimensions found in precast construction [18 in. to 24 in. (457 mm to 610 mm)]. Further, section size allowed the application of up to 15% of the gross section compression strength [with design concrete compression strength, f'_{dc} = 5.0 ksi (414 MPa)] as a constant axial load based on the available equipment in the laboratory. This range of applied axial load represents the majority of axial loads applied in previous lateral load testing of RC columns found in the literature (PEER 2020).

The height of the column test specimens at the lateral load application point, h_w was selected to result in the same moment-to-shear condition at the column-to-foundation interface as a full-height column in the first story of a typical building. Considering a realistic first-story height for a building of 12 ft (3.66 m) and that the column specimens were tested in a cantilever configuration, the specimen height to the lateral load application point was chosen to be half the story height [i.e., h_w= 6 ft (1.83 m)]. This corresponds to a moment-to-shear ratio of 3.6, which is within the typical range for previous column axial-flexural tests found in the literature (PEER 2020).

The column longitudinal (i.e., vertical) reinforcement ratio for the specimens was selected as 1.6% based on the range of typical reinforcement ratios found in the literature (most between 1.5% and 2.5%). This also satisfies the requirements in Chapter 18 of ACI 318-19 for minimum (1.0%) and maximum (6.0%) longitudinal reinforcement ratio for columns in special moment frames. The selected reinforcement ratio corresponded to eight No. 8 bars, four in the column corners and one at the centerline of each column face. The longitudinal reinforcement for all specimens had a specified yield strength, f_{syl} = 60 ksi (414 MPa).

The varied parameters included: (1) confinement type (strip versus reinforcing bar), (2) confinement layout (hoops/ties, single spiral, two spirals, two spirals out-of-phase), and (3) confinement reinforcement ratio Table 1 and Figure 4). Specimen RH-1.20 represented a state-of-the-practice (i.e., “control”) specimen using conventional reinforcing bar cross-ties (Figure 3A). The confinement reinforcement was determined based on the requirements in Section 18.7.5 of ACI 318-19 (ACI 2019), using reinforcing bar cross-ties with a specified yield strength, f_{syt} = 100 ksi (689 MPa) and a design concrete compression strength, f'_{dc} = 5 ksi (414 MPa). The confinement layout consisted of No. 4 hoops around the column longitudinal bars with overlapping No. 3 cross-ties connecting the bars on opposite column faces (Figure 4). Specimen 2SS-1.32 represented a corresponding strip-confined specimen with two concentric spirals (i.e., one outer square spiral around the perimeter and one inner circular spiral) and approximately the same confinement reinforcement ratio (Figure 3B). Specimen 2SSO-1.32 was identical to Specimen 2SS-1.32, except that the spirals were out-of-phase with one another. Specimen SST-1.18 featured an outer strip square spiral and strip cross-ties connecting the longitudinal bars on opposite faces, with approximately the same confinement ratio as the control Specimen RH-1.20. Specimen 2SS-0.98 featured the same layout as Specimen 2SS-1.32, but a reduced confinement ratio that was achieved by increasing the center-to-center spacing of the confinement steel, s_t. Finally, SS-1.15 used only one strip square spiral, with approximately the same confinement ratio as the control Specimen RH-1.20. The strip thicknesses and widths were selected to result in strip cross-sectional areas similar to either No. 3 or No. 4 reinforcing bar. This allowed for more direct comparisons to the confinement in conventional RC columns. All specimens used a clear cover of 1.5 in. (38.1 mm) to the outside edges of the confined region. As shown in Figure 3B, the strip reinforcement did not continue into the foundation of the specimen and there was a construction cold joint between the foundation and the column specimen (discussed further in the next section). Each column was directly wet-cast against the corresponding hardened foundation with continuous longitudinal reinforcement, but the combination of the cold joint and confinement discontinuity aimed to simulate a precast column base connection.

Table 2 compares each specimen to the relevant code requirements of ACI 318-19, including the center-to-center spacing of the confinement steel, s_t, the clear spacing of the confinement steel, s_{tc}, and the volumetric reinforcement ratio of the confinement steel, ρ_{st}. Bold cells indicate where a specimen violated a code requirement. The minimum volumetric confinement ratios were calculated per Table 18.7.5.4 of ACI 318-19, with the minimum volumetric confinement ratio for rectilinear hoops, $\rho_{st,min1}$ calculated as:

$$\rho_{st,min1} = 0.60\left(\frac{A_g}{A_{ch}} - 1\right)\frac{f'_{dc}}{f_{syt}} \quad (1)$$

where A_g is the gross cross-sectional area, A_{ch} is the cross-sectional area of the concrete core measured to the outside edges of the confinement reinforcement. This equation was adapted from the area-based ratio found in Table 18.7.5.4 of ACI 318-19 to a volumetric-based ratio. The minimum volumetric confinement ratio for circular spiral/hoops, $\rho_{st,min2}$ was calculated as follows:

$$\rho_{st,min2} = 0.45\left(\frac{A_g}{A_{ch}} - 1\right)\frac{f'_{dc}}{f_{syt}} \quad (2)$$

The unique geometry of the rectilinear spiral strips does not meet the strict definitions of either rectilinear hoops or circular/spiral hoops. As such, both minimum reinforcement ratios are included in Table 2 as a point of reference, with Eq (1) being more applicable and conservative. All specimens met the ACI 318-19 requirements except Specimen 2SS-0.98, which intentionally violated the center-to-center spacing, s_t, the clear spacing, s_{tc}, and the volumetric reinforcement ratio, ρ_{st} requirements.

Specimen Construction

The construction of each test specimen was performed in the laboratory and consisted of the following task sequence: (1) assembly of the foundation block reinforcement cage and formwork, (2) fabrication of the column cage, including strip bending for the specimens with strip spiral confinement, (3) integration of the column cage with the foundation block, (4) casting of the foundation block, and (5) assembly of column formwork and casting of the column test specimen.

An arbor press was used to bend the high-strength coiled steel strip into the continuous spiral confinement for the column cages (Figure 5A). A specialized aluminum jig was designed and integrated with the arbor press to act as a press brake and control the bend radius and angle. This allowed for repeatability and consistency throughout the bending process. To fabricate the spiral confinement, the coiled steel strip was continuously fed into the arbor press using the decoiler (Figure 1) and bent at predetermined spacings to result in the specified out-to-out dimensions of the confined region in the column. In addition, the angle of the aluminum jig was set to create the desired pitch/spacing for the strip spiral. After the bending of the strip, the column cage was assembled using a specially designed horizontal rig in the laboratory (Figure 5A and Figure 5B). The two ends of the rig were constructed with plywood and functioned as templates for the placement of the column longitudinal reinforcement inside the strip confinement region. Four threaded rods were used to couple the two ends of the rig together and ensure rigid body movement as the column cage was assembled. The entire rig was suspended horizontally between two steel columns in the laboratory using a long center dowel rod, which allowed for rotation of the rig about its center axis. This free rotation eased the placement of the strip spiral on the rig for the final assembly of the column cage. In the long-term, it is envisioned that this process could be automated for accelerated fabrication.

After fabrication, the bottom portion of the column cages were placed inside the assembled foundation block cage and formwork (Figure 5D). The foundation block was poured first to result in a construction cold joint at the column-to-foundation interface. Figure 5E shows three completed specimens after concrete casting and removal of the formwork (foreground).

Concrete Properties

The target concrete compressive strength for the column specimens was f'_{dc} = 5 ksi (414 MPa). This was selected along with the column cross-section dimensions so that the experimental testing frame could apply the desired axial load of 15% of the gross section compressive strength.

Table 1 summarizes the measured concrete compressive strength, f'_c and the measured concrete elastic modulus, E_c on the day that each column specimen was tested. For each column specimen, the concrete compressive strength, f'_c was determined by testing 3 x 6 in. (76.2 x 152 mm) cylinder samples (average of three) using a universal testing machine according to the procedures defined in ASTM C39. The nominal cylinder cross sectional area was used to calculate the concrete stress from the measured load. The concrete elastic modulus, E_c was calculated according to ASTM C469, using the measured concrete compressive strains [via an averaging axial extensometer with a 2 in. (50.8 mm) gauge length] in the linear-elastic range of the cylinder samples. Note that for Specimen 2SSO-1.32, strain data was only available for two cylinder samples.

Steel Properties

Material testing according to ASTM A370 was performed on the steel reinforcing bar and strip using a universal testing machine (Table 3 and Figure 6).

Full cross-section reinforcing bar samples were tested with an 8 in. (203 mm) length between crosshead grips, with a 2-in. (50.8-mm) extensometer positioned approximately in the middle of this length. The reported bar strains up to the peak stress, f_u were measured using this extensometer. Beyond the peak stress, f_u, the incremental strains were approximated based on the incremental change in the distance between the crossheads.

The steel strip samples were machined to a dog bone shape with a reduced width of 0.5 in. (12.7 mm) over a 3-in. (76.2-mm) length to allow the placement of the available 2-in. (50.8-mm) extensometer. The reported strip strains up to 0.04 were measured using the extensometer, with incremental strains beyond this determined based on the incremental change in displacement of the crossheads.

Since the high-strength deformed reinforcing bar [ASTM A1035 #3 and #4 (Metric #10 and Metric #13)] and the DP 980/700 strip steel did not have a yield plateau, the 0.2% offset method was used to determine the yield strength. The yield strength of the ASTM 615 #8 (Metric #25) longitudinal bar was determined based on the distinctive yield plateau. A linear regression of the measured stress-strain curve was used to determine the elastic modulus for each sample.

Test Setup and Loading Protocol

Figure 7A and Figure 7B depict an elevation view schematic and 3D rendering, respectively, of the testing setup in the laboratory, with Figure 7C and Figure 7D showing photographs of a specimen in the test setup prior to testing. As shown in Figure 3 and Figure 7, each test specimen consisted of a foundation block tied down to the strong floor, the column test region, and an enlarged loading cap for application of the axial and lateral loads.

The lateral load on each specimen was applied using a 220-kip (979-kN) capacity servo-controlled hydraulic actuator attached to a near-rigid steel reaction frame and connected to the column at the end cap region (Figure 7). The target loading protocol was consistent with the *ACI T1.1-01 Acceptance Criteria for Moment Frames Based on Structural Testing* (ACI 2001) testing protocol and is summarized in Table 4. Four load-controlled series were first applied to the columns in their linear-elastic range, with three fully reversed cycles per series. Directly following the load-controlled series, displacement-controlled series (with three fully reversed cycles per series) were conducted with target drifts increasing by approximately 1.5 times the target drift of the prior series up to the required 3.5% validation drift prescribed by the ACI T1.1-01 acceptance criteria. Additional series were continued until the actuator ran out of stroke or failure of the specimen (with failure defined as the measured load dropping below 75% of the peak strength, V_p in both loading directions). The same loading protocol was applied to all six specimens. The only exception is that for Specimen RH-1.20 and 2SS-1.32 the fourth load cycle was not implemented as the specimen was already at the displacement limit for the first displacement control cycle. Simultaneously, two 2,220-kN (250-ton) hydraulic jacks on top of the specimen applied the constant, concentric axial load by reacting against a steel loading beam. The magnitude of the applied load was 15% of the gross section compression strength, with this value based on the test day concrete compressive strength. This ranged from 340 – 365 kips (1,510 – 1620 kN). The vertical axial force from the hydraulic jacks was resisted by high-strength, 2.5-in. (63.5-mm) diameter rods at each end of the loading beam. These threaded rods were anchored through two RC reaction blocks that were tied down to the laboratory strong floor. In a pocket under each reaction block, a steel rocker plate allowed for the rotation of the rods as the column was laterally displaced. An external lateral bracing frame was used to restrain any out-of-plane movement [i.e., left-right in Figure 7A] of the column specimen during loading.

The behavior of each test specimen was monitored using a suite of sensors as shown in Figure 8. To measure displacements, a combination of spring return linear position sensors (PS; BEI Sensors, 9600 Series) and string potentiometer displacement sensors (DS; MD Totco 1850-002) were used. Rotations were measured using clinometers (RS; Measurement Specialties, AccuStar Electronic Clinometer). The lateral load was measured using a load cell (internal to the actuator) and the axial load was measured using pressure transducers.

EXPERIMENTAL RESULTS AND DISCUSSION

Table 5 provides the initial stiffness, K_i (measured as the average secant stiffness to the peak points of the three cycles of the series corresponding to 75% of the peak lateral load, V_p for each specimen), the lateral load at initial column cracking, V_c, the peak lateral load, V_p, the lateral load at the validation-level drift (i.e., Δ = 3.5%), V_v, and the drift at peak lateral load, Δ_p. Figure 9 shows the lateral load versus displacement (and drift) behavior for each specimen and Figure 10 shows the envelope of this behavior. Rocking and slip of the foundation were removed from the measurements.

Failure of the specimens, except for Specimen SS-1.15, could not be achieved as the actuator ran out of stroke, with failure being defined as a lateral load less than 75% of the peak lateral load, V_p in each loading direction per ACI T1.1-01. It is expected that Specimen SS-1.15 would be the most likely specimen to fail as it was confined by only a single strip spiral, meaning that the middle bars had little restraint from buckling. Barbachyn et al. (2023) found that in an eight-bar layout, the middle bars were not adequately restrained against buckling and thus recommended the use of two strip spirals. Specimen 2SS-0.98, which had the smallest confinement reinforcement ratio and violated the ACI center-to-center spacing, s_t, clear spacing, s_{tc}, and volumetric confinement reinforcement ratio, ρ_{st} requirements (Table 2), had a load drop of 29.8% in the positive direction of the third cycle of the last series, but the third cycle in the negative direction could be not completed.

The strip-confined specimens exhibited similar peak strengths as compared to the control specimen, with peak strengths between -0.36% and +1.43% of the control column strength in the positive loading direction and between -7.54% and -2.36% in the negative loading direction. Table 6 compares the peak lateral strength, V_p to the nominal lateral strength, E_n (calculated using the specified material strengths), and the probable lateral strength, E_{pr} (calculated using the measured material strengths). All specimens had a peak lateral strength that exceeded both the nominal and probable lateral strengths. For the control specimen, the ratio of the peak lateral strength to the probable lateral strength (V_p/E_{pr}) was 1.09 in the positive loading direction and 1.16 in the negative loading direction. In comparison, the average ratio for the strip-confined specimens was 1.06 in both the positive and negative directions. Varying the strip confinement layout (single spiral, single spiral with ties, two spirals, two spirals out-of-phase) and confinement reinforcement ratio had negligible impact on the peak lateral strength. Overall, the peak strength of the strip-confined specimens was comparable to that of a rebar-confined control specimen and exceeded analytical predictions for the lateral strength, even for Specimen 2SS-0.98 which violated the ACI minimum reinforcement ($\rho_{st,min1}$) as well as the center-to-center spacing and clear spacing requirements for confinement steel.

The initial stiffness, K_i of all of the strip-confined specimens exceeded that of the control specimen in both loading directions (Table 5). This was more pronounced in the positive loading direction where the average stiffness of the strip-confined specimens was 152 kips/in (17,100 kN/mm) as compared to the rebar-confined control specimen at 97.7 kips/in (11,000 kN/mm), i.e., a 55.2% increase. In the negative loading direction, the average stiffness of the strip-confined specimens was 19.3% higher than the rebar-confined specimen. For all of the strip-confined specimens, the stiffness in the negative loading direction was less than that in the positive loading direction. The specimens with the greatest drops used a single spiral: Specimen SST-1.18 (19.3% drop) and Specimen SS-1.15 (14.0% drop). In contrast, Specimen 2SSO-1.32, with two out-of-phase spirals had the least drop in stiffness (6.04%). As a point of comparison, Specimen RH-1.20 had a 14.6% increase in stiffness. This indicates that there may be some directionality associated with the orientation of the spiral and the loading direction, and that two out-of-phase spirals may provide the most consistent stiffness. This is an area for future research. The lateral load at initial column cracking, V_c was similar among all of the tested specimens (Table 5).

Importantly, all specimens met the ACI T1.1-01 criterion that the lateral load at the third complete cycle for the validation drift ratio of 3.5%, V_v was not below 75% of the peak load, V_p (Table 5). This indicates that strip-confinement has the potential to provide the necessary strength and ductility for high seismic regions.

The lateral load versus displacement (and drift) behavior of the specimens (Figure *9* and Figure *10*) indicate that that the loss of cover at the peak load had a larger effect on the behavior of the rebar-confined specimen as compared to the strip-confined specimen. This supports the expected benefit from larger confined core area in strip confined columns. Table *5* compares the lateral load at validation-level drift to the peak load, V_v/V_p showing generally greater values for the strip-confined specimens, further indicating improved residual strength behavior using strip confinement.

After testing was completed, the specimens were excavated at their base to better understand any longitudinal bar buckling or confinement steel rupture (Figure 11). In control Specimen RH-1.20, there was no visible buckling of the longitudinal bars. In Specimen 2SS-1.32, which is most comparable to the control specimen, there was also no visible buckling of the longitudinal bars. This indicates that the two strip spirals is able to provide a similar restraint to bar buckling as the conventional deformed reinforcing bar hoops and ties. Note that Specimen 2SS-1.32 had a slightly higher volume of confinement reinforcement than Specimen RH-

1.20 due to the confinement geometry for the two-strip spiral layout (i.e., one inner circular spiral and one outer square spiral). In Specimen 2SSO-1.32, which used the same volume of strip spiral reinforcement as Specimen 2SS-1.32 but had the inner and outer spirals out-of-phase, there was significant corner bar buckling on the positive loading side of the specimen, potentially indicating that out-of-phase spirals reduce the confinement performance in restraining buckling. Specimen SST-1.18, which featured a single strip spiral and strip ties, did not show any significant longitudinal bar buckling, indicating that this layout is another viable option that provides comparable restraint to bar buckling as conventional deformed reinforcing bar hoops and ties. Specimen 2SS-0.98, which violated the center-to-center spacing, s_t, the clear spacing, s_{tc}, and the volumetric confinement reinforcement ratio, ρ_{st} requirements of ACI 318-19 (Table 2), had noticeable bar buckling of the extreme middle and corner longitudinal bars. This indicates that maintaining the current ACI confinement requirements for the steel strip is likely appropriate. In Specimen SS-1.15 with the single outer spiral, significant buckling was observed in both the corner and middle extreme longitudinal bars. The buckling of the corner longitudinal bars was more pronounced on the negative loading side. This was expected, as Barbachyn et al. (2023) had previously found that a single perimeter spiral did not sufficiently restrain longitudinal bars from buckling, particularly the middle bars. The steel strip did not rupture in any of the specimens.

CONCLUSIONS

This report presents the measured and observed behaviors of six full-scale RC columns subjected to reversed-cyclic lateral loading and a constant concentric axial compression load. The behavior of columns confined using dual-phase, high-strength [100 ksi (690 MPa) yield strength] steel strips is compared with the behavior of a control specimen confined using deformed reinforcing bars [i.e., using 100 ksi (690 MPa) yield strength ties]. The varied parameters included: (1) confinement type (strip versus reinforcing bar): (2) confinement layout (hoops/ties, single spiral, two spirals, two spirals out-of-phase); and (3) confinement ratio. The major conclusions are as follows:

1. The peak lateral strength of the strip-confined specimens was comparable to that of the rebar-confined control specimen and exceeded analytical predictions for lateral strength.
2. The initial lateral stiffness of the strip-confined specimens exceeded that of the rebar-confined control specimen, with the average stiffness of the strip-confined specimens being 55.2% higher in the positive loading direction and 19.3% higher in the negative loading direction.
3. The strip-confined specimen with out-of-phase spirals exhibited more consistent stiffness among the two loading directions as compared to the other strip-confined specimens. This may indicate directionality

associated with the orientation of the spiral and that there are advantages in using two, out-of-phase spirals. This is an area for future research.

4. All specimens met the ACI T1.1-01 criteria that the lateral load at the third complete cycle for the validation drift ratio of 3.5% was not below 75% of the peak load in each direction, indicating that strip confinement has the potential to provide the necessary lateral strength and ductility for RC columns in high seismic regions.
5. The strip-confined specimens demonstrated improved residual strength behavior compared to the rebar-confined specimen, indicating that the strip was able to provide a larger confined core area.
6. In a configuration with 8 longitudinal bars, an outer square strip spiral and an inner circular strip spiral is recommended, as compared to a single outer square strip spiral, to better restrain longitudinal bar buckling.
7. In a configuration with 8 longitudinal bars, an outer square strip spiral with strip cross-ties behaved similarly to a two-strip spiral layout and is a viable alternative. However the individual ties were more labor intensive to fabricate as compared to the spirals.
8. The center-to-center spacing, clear spacing, and minimum reinforcement ratio requirements of ACI 318-19 are likely appropriate for strip confinement.

Overall, this research indicates that steel strip confinement is a viable strategy for earthquake-resistant design of RC columns. Additional experimental research is necessary to investigate the impact of varying axial compression on behavior. Important future research directions include developing validated numerical models and simplified analytical expressions that can predict the lateral behavior of strip-confined columns for design.

ACKNOWLEDGMENTS

This report is based on work supported by an American Concrete Institute Foundation (ACIF) Concrete Research Council Grant. The authors are also grateful for support from a University of Notre Dame Recovery and Resilience Grant. The authors gratefully acknowledge the support of ACIF Program Directors Ann Masek and Tricia Ladely and ACI Committee 550 Representatives Suzanne Altman and Larbi Sennour. The support and guidance from the Industry Advisory Group is also acknowledged. This group includes: Don Meinheit (Wiss, Janney, Elstner Associates, Inc.), Clay Putnam (Metromont Corp.), Mark Sarkisian and Austin Devin (Skidmore, Owings & Merrill), Ted Zoli (HNTB Corp.), Adam Reihl (StresCore, Inc.), Matt Ballain (Coreslab Structures, Inc.), Nathan Krause and Bruce Hopkins (Kerkstra Precast, Inc.), and Jared Brewe (PCI). The authors gratefully acknowledge

ArcelorMittal for its generous donation of steel product. Without this donation, the work would not have been possible. Any findings, conclusions, or recommendations in this report are those of the authors and do not necessarily represent the views of the organizations/individuals acknowledged.

NOTATION:

A_{ch} = cross-sectional area of concrete core measured to the outside edges of the confinement reinforcement

A_g = gross cross-sectional concrete area

d_b = reinforcing bar diameter

E_c = measured concrete elastic modulus

E_n = nominal lateral resistance

E_{pr} = probable lateral resistance

E_s = measured steel elastic modulus

f'_{dc} = design concrete compressive strength

f'_c = measured concrete compressive strength

f_{sy} = specified yield strength

f_{syl} = specified longitudinal steel yield strength

f_{syt} = specified confinement steel yield strength

f_u = measured steel peak strength

f_y = measured yield strength

f_{yl} = measured longitudinal steel yield strength

f_{yt} = measured confinement steel yield strength

f_u = measured steel peak strength

h_w = height of the specimen

K_i = initial stiffness

n_b = number of longitudinal bars

s_t = center-to-center spacing of confinement steel

s_{tc} = clear spacing of confinement steel

t_s = steel strip thickness

V_c = lateral load at initial column cracking

V_p = peak lateral load

V_v = lateral load at validation-level drift

w_s = steel strip width

Δ = drift

Δ_p = drift at peak lateral load

ε_y = measured steel strain at yield

ε_r = measured steel strain at rupture

ε_u = measured steel strain at peak strength

ρ_{sl} = longitudinal steel reinforcement ratio

ρ_{st} = volumetric reinforcement ratio of confinement steel

REFERENCES

ACI Committee 318, "Building Code Requirements for Structural Concrete (ACI 318-19) and Commentary (ACI 318R-19)," American Concrete Institute, Farmington Hills, MI, 2019, 624 pp.

ACI Committee 93, "T1.1-01 Acceptance Criteria for Moment Frames Based on Structural Testing." American Concrete Institute, Farmington Hills, MI, 2001, 10 pp.

ASTM C39/C39M-21, "Standard Test Method for Compressive Strength of Cylindrical Concrete Specimens." ASTM International, West Conshohocken, PA, 2021, 8 pp.

ASTM C469/C469M-22, "Standard Test Method for Static Modulus of Elasticity and Poisson's Ratio of Concrete in Compression." ASTM International, West Conshohocken, PA, 2022, 6 pp.

ASTM A370-22, "Standard Test Methods and Definitions for Mechanical Testing of Steel Products." ASTM International, West Conshohocken, PA, 2022, 51 pp.

ASTM E111-17, "Standard Test Method for Young's Modulus, Tangent Modulus, and Chord Modulus." ASTM International, West Conshohocken, PA, 2017, 7 pp.

Barbachyn, S.B., O'Donnell, A., Thrall, A.P., and Kurama, Y.C., 2023, "Axial load behavior of reinforced concrete columns with high-strength steel coiled strips as confinement." *PCI Journal*, V. 86, No. 5, pp. 21-41.

Kidder, F. E. and T. Nolan. *Building Construction and Superintendence.* William T. Comstock, New York, NY, 1911.

PEER, "PEER Structural Performance Database," Pacific Earthquake Engineering Research Center, 2020. < https://nisee.berkeley.edu/spd/index.html> (accessed Jan. 30, 2020).

Rizwan, M., Khan, S.A., Ilyas, M., and Hussain, R.R., 2016, "Modelling steel-strip-confined reinforced-concrete columns." *Structures and Buildings*, V. 169, No. 4, pp. 245-256.

Rizwan, M., 2009, *Performance of RC Structures under Earthquake Loading*. Ph.D. Dissertation, University of Engineering and Technology, Lahore Pakistan, 2009.

Shafqat, A. and A. Ali., 2012, "Lateral Confinement of RC Short Column." *Science International (Lahore)*, V. 24, No. 4, pp. 371-379.

Tahir, M.F., Khan, Q.U.Z., and Ahmad, A., 2015, "Effect of Concrete Strength on Behavior of Strip Confined Columns." *Technical Journal, University of Engineering and Technology Taxila,* V. 19, No. II, pp. 28-34.

TABLES AND FIGURES

List of Tables:

Table 1 - Test Specimen Details

[1]Column Specimen	f_c' (ksi)	E_c (ksi)	Longitudinal Reinforcement				Confinement Reinforcement						
			n_b	U.S. Size	f_{yl} (ksi)	ρ_{sl} (%)	Type	d_b (in.)	w_s (in.)	t_s (in.)	s_t (in.)	f_{yt} (ksi)	ρ_{st} (%)
RH-1.20	**5.73**	**7.11**	8	#8	64.9	1.58	**rebar hoops w/cross-ties**	**0.50/ 0.38**	**N/A**	**N/A**	**5.00**	**122/ 133**	**1.20**
2SS-1.32	5.69	6.89					two strip spirals	N/A	2.75/ 2.00[2]	0.08/ 0.06[2]	5.00	101/ 105	1.32
2SSO-1.32	5.85	5.51					two strip spirals (out-of-phase)		2.75/ 2.00[2]	0.08/ 0.06[2]	5.00	101/ 105	1.32
SST-1.18	6.11	7.26					one strip spiral with cross-ties		2.75/ 2.00[3]	0.08/ 0.06[3]	5.00	101/ 105	1.18
2SS-0.98	5.91	7.43					two strip spirals		2.75/ 2.00[2]	0.08/ 0.06[2]	6.75	101/ 105	0.98
SS-1.15	5.84	7.29					one strip spiral		2.75	0.08	4.00	101	1.15

Note: f_c'= measured concrete compressive strength on column test day (3x6 in. cylinders); E_c= measured concrete elastic modulus on column test day (3x6 in. cylinders); n_b= number of longitudinal bars; f_{yl}= measured longitudinal steel yield strength; ρ_{sl}= longitudinal steel reinforcement ratio; d_b= reinforcing bar diameter; w_s= steel strip width; t_s= steel strip thickness; s_t= center-to-center spacing of confinement steel; f_{yt}= measured confinement steel yield strength; ρ_{st}= volumetric reinforcement ratio of confinement steel. 1 ksi=6.89 MPa; 1 in.=25.4 mm; N/A=not applicable.

[1]first term denotes confinement reinforcement type and layout (RH=reinforcing bar hoops; 2SS=two strip spirals; 2SSO=two strip spirals that are out-of-phase; SST=one strip spiral with cross-ties); second term denotes confinement volumetric ratio as a percentage;

[2]dimension for outer spiral/dimension for inner spiral

[3]dimension for strip spiral/dimension for strip ties

bold=control column

Table 2 - ACI 318-19 Confinement Requirements

[1]Column Specimen	ACI 318-19 Requirement					Specimen Confinement Reinf.		
	[2]$s_{t,max}$ (in.)	[3]$s_{tc,min}$ (in.)	[4]$s_{tc,max}$ (in.)	[5]$\rho_{st,min1}$ (%)	[6]$\rho_{st,min2}$ (%)	s_t (in.)	s_{tc} (in.)	ρ_{st} (%)
RH-1.20	5.00	0.50	N/A	1.15	N/A	5.00	4.50	1.20
2SS-1.32			3.00		0.864	5.00	2.25	1.32
2SSO-1.32						5.00	2.25	1.32
SST-1.18						5.00	2.25	1.18
2SS-0.98						**6.75**	**4.00**	**0.98**
SS-1.15						4.00	1.25	1.15

Note: s_t= center-to-center spacing of confinement steel; s_{tc}= clear spacing of confinement steel; ρ_{st}= volumetric reinforcement ratio of confinement steel. 1 in.=25.4 mm. N/A=not applicable.

[1]first term denotes confinement reinforcement type and layout (RH=reinforcing bar hoops; 2SS=two strip spirals; 2SSO=two strip spirals that are out-of-phase; SST=one strip spiral with cross-ties); second term denotes confinement volumetric ratio as a percentage;

[2]from Section 18.7.5.3 of ACI 318-19

[3]from Section 25.7.2.1(a) of ACI 318-19 with nominal coarse aggregate size of 3/8 in.

[4]from Section 25.7.3.1(b) of ACI 318-19 for spirals

[5]adapted from Expression (a) in Table 18.7.5.4 of ACI 318-19 for rectilinear hoops

[6]from Expression (d) in Table 18.7.5.4 of ACI 318-19 for spirals and circular hoops

[7]center-to-center or clear spacing (i.e., pitch) of outside and inside strip spirals

bold values=specimen parameters that did not meet one or more ACI 318-19 requirements; For minimum reinforcement ratios, $\rho_{st,min1}$ governs for spiral strips as opposed to $\rho_{st,min2}$ as the spiral strips do not meet the strict definition of spirals in ACI 318-19.

Table 3 - Column Reinforcement Properties

Property	Confinement Reinforcement				Longitudinal Reinforcement
Specification	DP 980/700	DP 980/700	ASTM A1035	ASTM A1035	ASTM A615
Size	0.06x2.00 in.	0.08x2.75 in.	U.S. #3	U.S. #4	U.S. #8
f_{sy} (ksi)	100	100	100	100	60
f_y (ksi)	105	101	133	122	64.9
ε_y (%)	0.640	0.660	0.650	0.650	0.270
E_s (ksi)	24000	21900	29300	27500	26100
f_u (ksi)	142	137	165	157	104
ε_u (%)	7.68	8.03	5.02	5.32	10.8
ε_r (%)	11.5	12.5	8.08	9.56	17.8

Note: f_{sy}= specified yield strength; f_y= measured yield strength; ε_y= measured steel strain at yield; E_s = measured steel elastic modulus; f_u = measured steel peak strength; ε_u= measured steel strain at peak strength; ε_r= measured steel strain at rupture. 1 in.=25.4 mm; 1 ksi=6.89 MPa

Table 4 - Lateral Testing Protocol

Series	Lateral Load (kips)	[1]Column Drift (%)	Column Disp. (in.)	No. of Cycles
1	10	-	-	3
2	20			3
3[2]	30			3
4[3]	40			3
5[3]	-	0.333	0.240	3
6		0.500	0.360	3
7		0.750	0.540	3
8		1.10	0.792	3
9		1.60	1.15	3
10		2.40	1.73	3
11		3.50	2.52	3
12		4.50	3.24	3
13		5.50	3.96	3

Note: [1]Column lateral displacement at line of load application divided by height from top of foundation. 1 kip = 4.45 kN; 1 in.=25.4 mm

Table 5 - Experimental Results

Measured Property		Specimen[1]					
		RH-1.20	2SS-1.32	2SSO-1.32	SST-1.18	2SS-0.98	SS-1.15
Positive Loading	K_i (kips/in.)	97.7	146	149	161	152	150
	V_c (kips)	35.0	34.1	39.2	34.1	37.4	36.0
	V_p (kips)	83.6	83.7	84.7	84.0	84.8	83.3
	V_v (kips)	73.7	77.1	75.2	78.2	77.2	70.2
	V_v/V_p	0.882	0.921	0.888	0.931	0.910	0.843
	Δ_p (%)	2.45	1.59	1.36	2.20	1.35	1.34
Negative Loading	K_i (kips/in.)	112	131	140	130	138	129
	V_c (kips)	-29.5	-31.9	-32.2	-27.7	-31.8	-28.3
	V_p (kips)	-88.8	-86.7	-82.1	-82.7	-84.0	-85.3
	V_v (kips)	-81.7	-80.9	-75.6	-76.2	-79.5	-76.9
	V_v/V_p	0.920	0.933	0.921	0.921	0.946	0.902
	Δ_p (%)	-1.93	-1.52	-1.40	-3.44	-3.44	-1.57

Note: K_i= initial stiffness; V_c= lateral load at initial column cracking; V_p= peak lateral load; V_v= lateral load at validation-level drift (i.e., Δ = 3.5%); Δ_p= drift at peak lateral load. 1 kip = 4.45 kN; 1 in.=25.4 mm;

[1]first term denotes confinement reinforcement type and layout (RH=reinforcing bar hoops; 2SS=two strip spirals; 2SSO=two strip spirals that are out-of-phase; SST=one strip spiral with cross-ties); second term denotes confinement volumetric ratio as a percentage

Table 6 - Lateral Load Comparison

[1]Column Specimen	V_p (kips)	E_n (kips)	E_{pr} (kips)	$\frac{V_p}{E_{pr}}$
RH-1.20	+83.6/-88.8	70.8	76.5	1.09/-1.16
2SS-1.32	+83.7/-86.7	72.7	78.2	1.07/-1.11
2SSO-1.32	+84.7/-82.1		79.3	1.06/-1.04
SST-1.18	+84.0/-82.7		81.0	1.04/-1.02
2SS-0.98	+84.8/-84.0		79.7	1.06/-1.05
SS-1.15	+83.3/-85.3		79.2	1.05/-1.08

Note: V_p= peak lateral load (for the positive, + and negative, - loading directions); E_n=nominal lateral resistance; E_{pr}=probable lateral resistance; 1 kip = 4.45 kN;
[1]first term denotes confinement reinforcement type and layout (RH=reinforcing bar hoops; 2SS=two strip spirals; 2SSO=two strip spirals that are out-of-phase; SST=one strip spiral with cross-ties); second term denotes confinement volumetric ratio as a percentage

List of Figures:

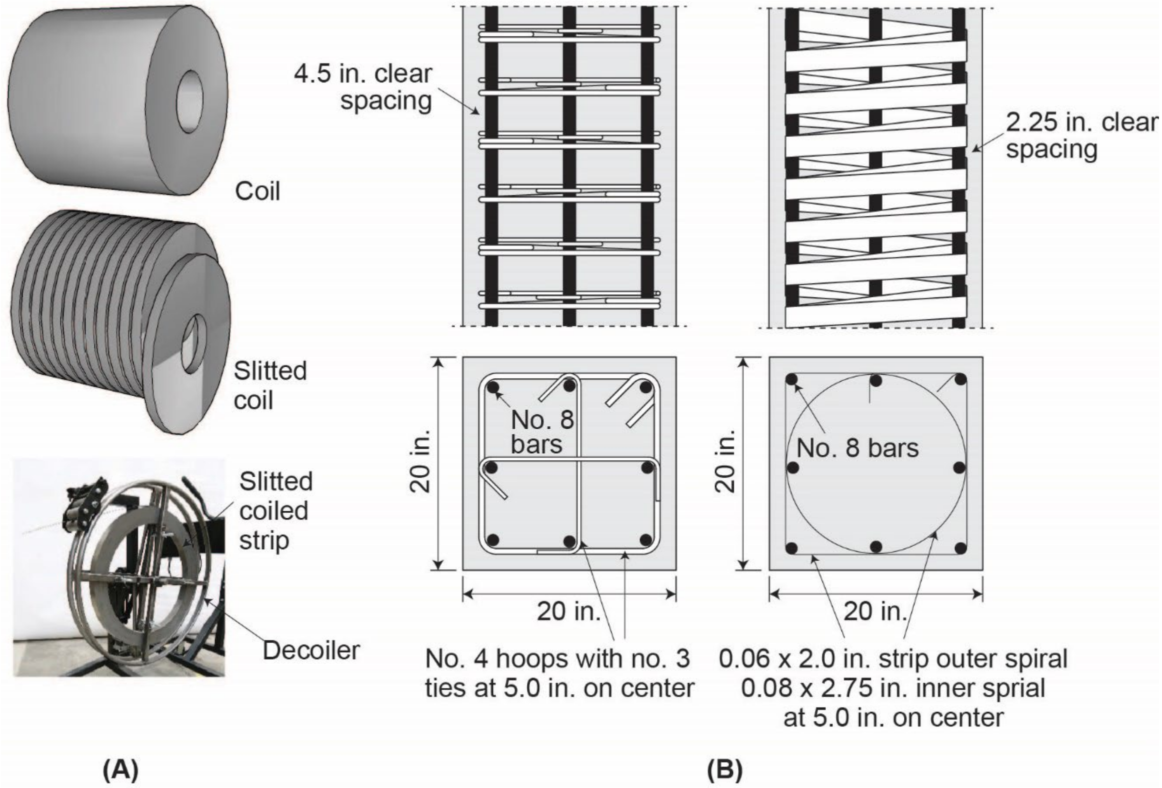

Figure 1 - High-strength steel strip reinforcement: (A) coil and strip and (B) hoop reinforcing bar (left) versus spiral strip (right) confinement for square column. Adapted from Barbachyn et al. (2023).

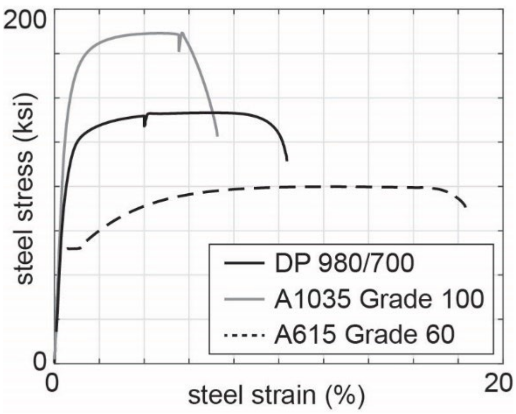

Figure 2 - Comparison of stress-strain behavior for DP 980/700 steel and reinforcing bar. Reprinted from Barbachyn et al. (2023).

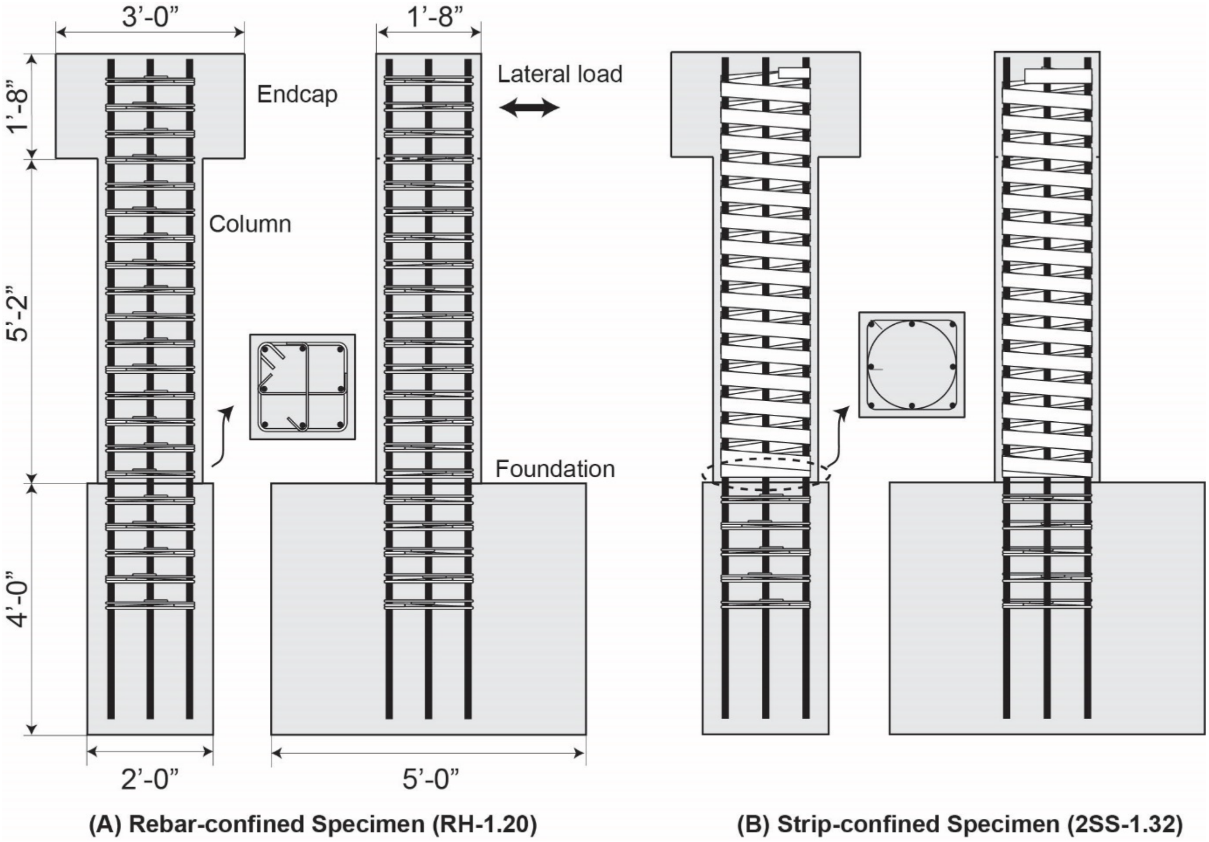

Figure 3 - Column specimens: (A) Rebar-confined specimen RH-1.20 and (B) Example strip-confined specimen 2SS-1.32.

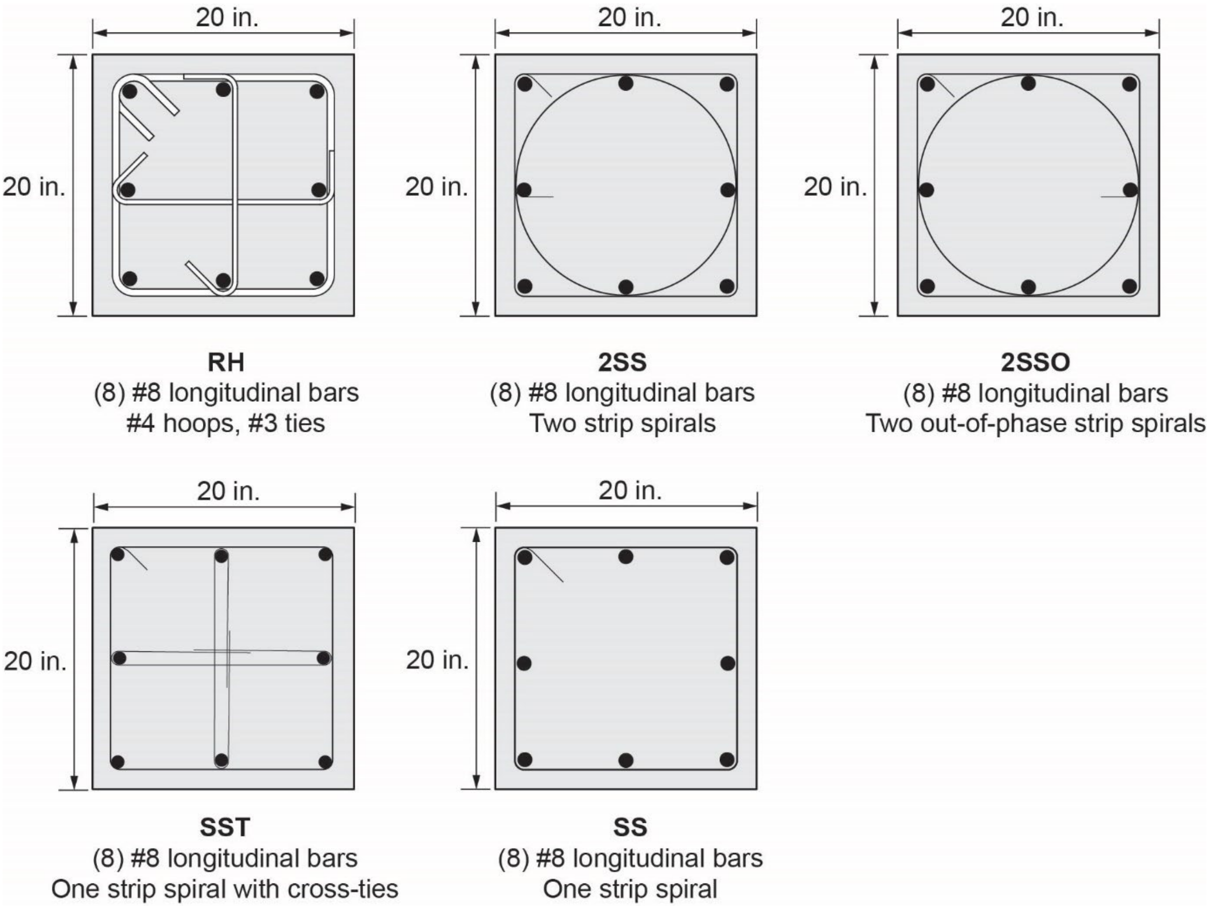

Figure 4 - Column confinement layouts.

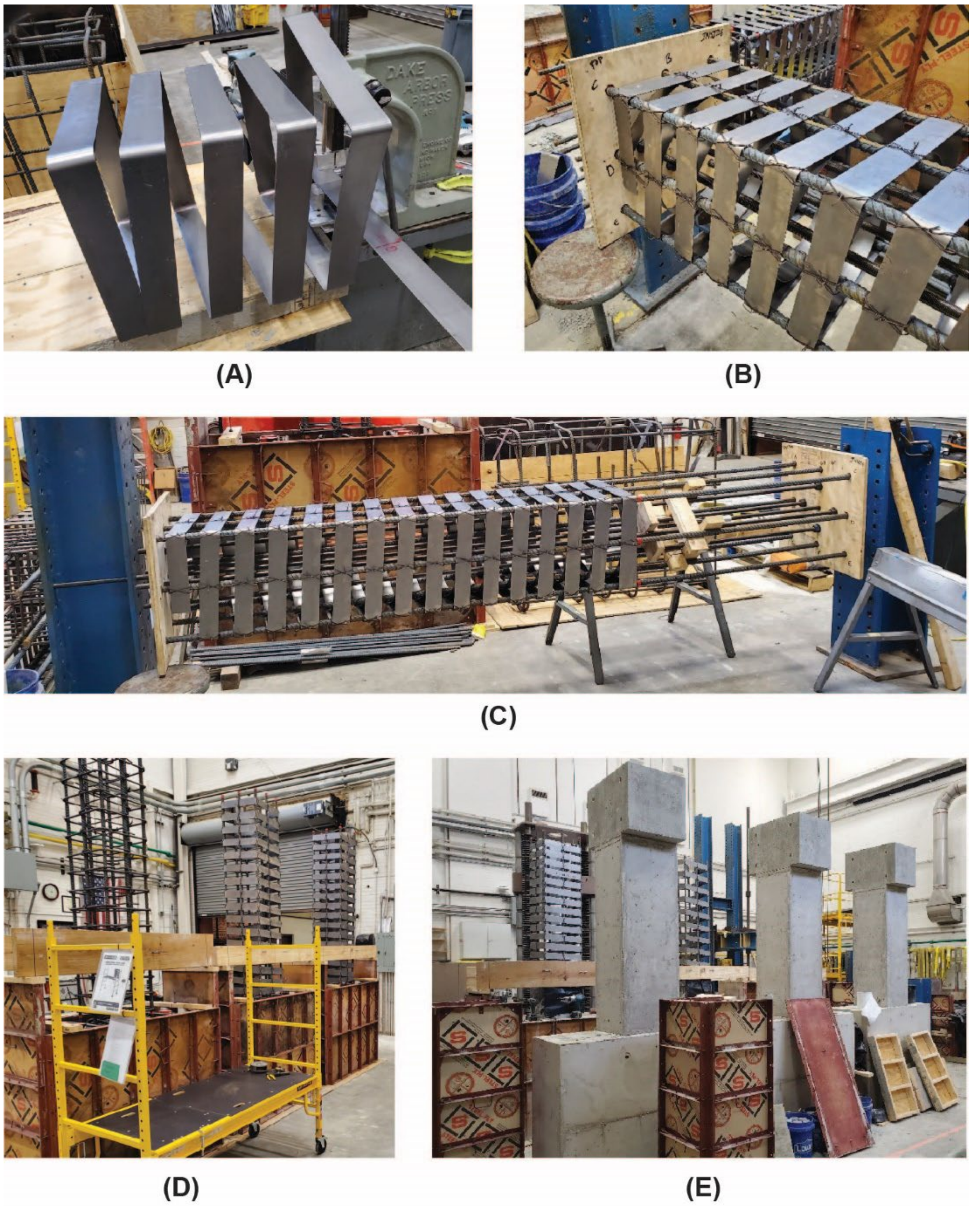

Figure 5 - Specimen construction: (A) bending strip via an arbor press, (B) bent strip tied to longitudinal rebar in rig, (C) complete strip spiral in rig, (D) rebar-confined and strip-confined specimens prior to casting of the foundation, with foundation formwork in place, and (E) fully cast specimens (foreground) and strip-confined specimens ready to be cast (background).

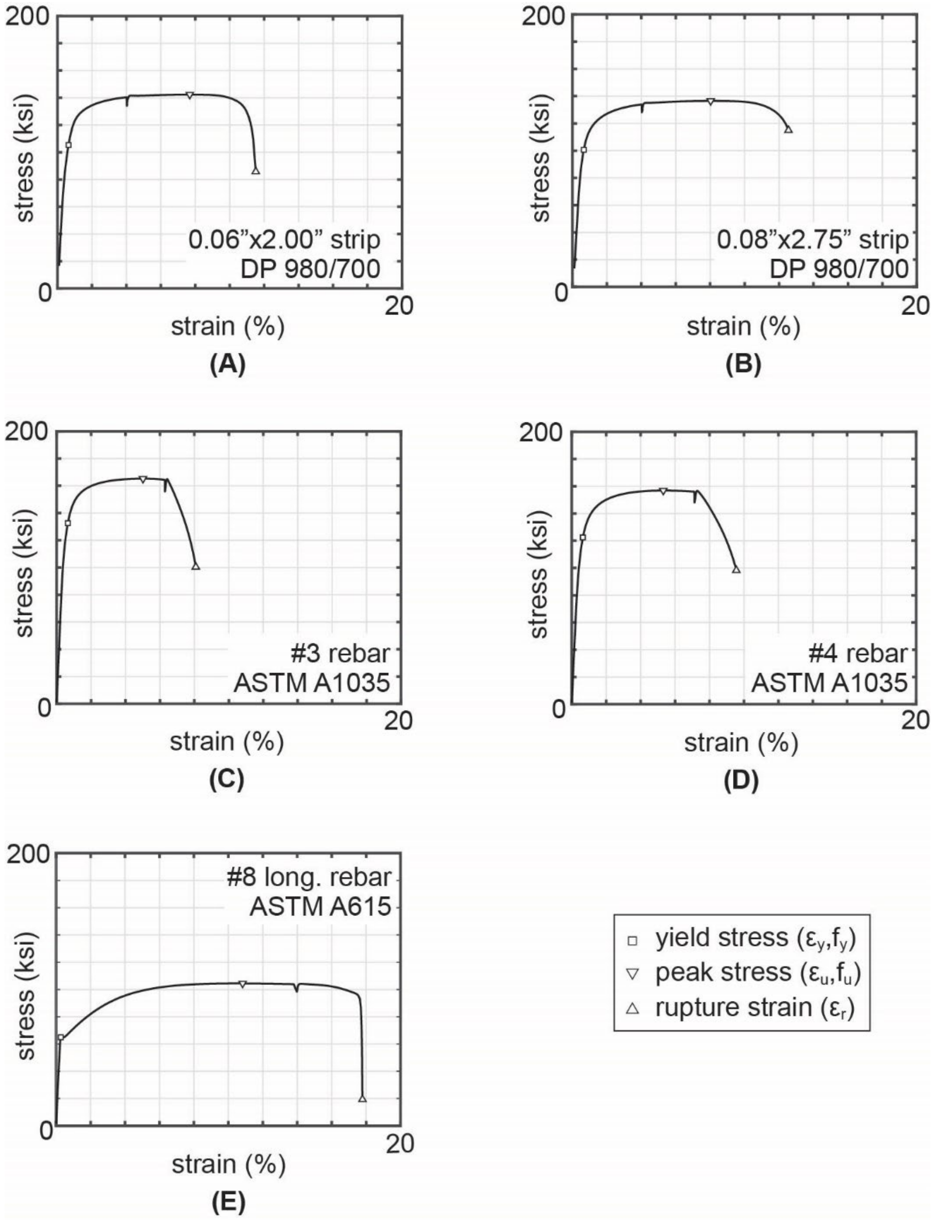

Figure 6 - Measured reinforcing steel stress versus strain behavior.

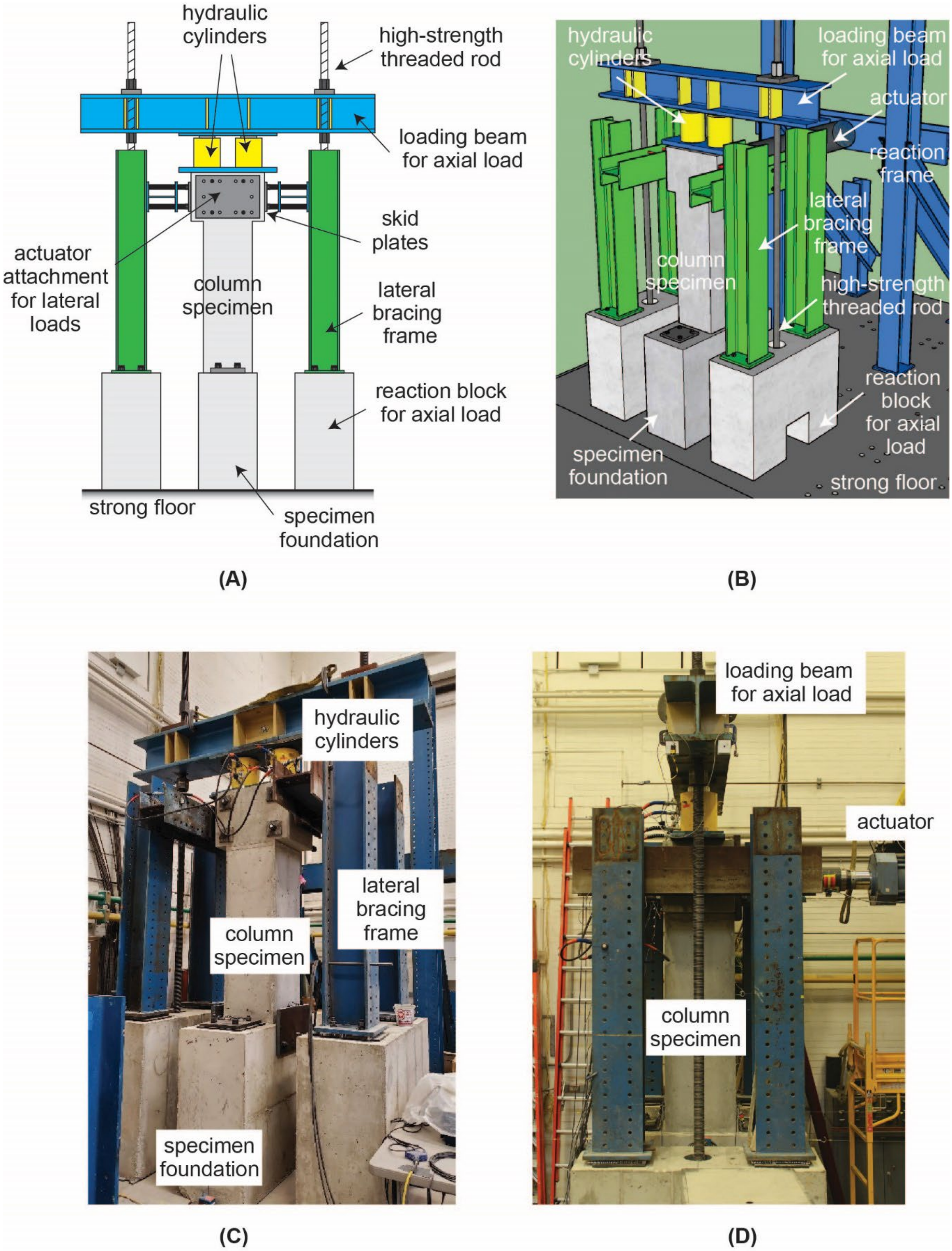

Figure 7 - Test Setup: (A) elevation view rendering, (B) 3D rendering, (C) specimen prior to testing, and (D) specimen prior to testing in side view.

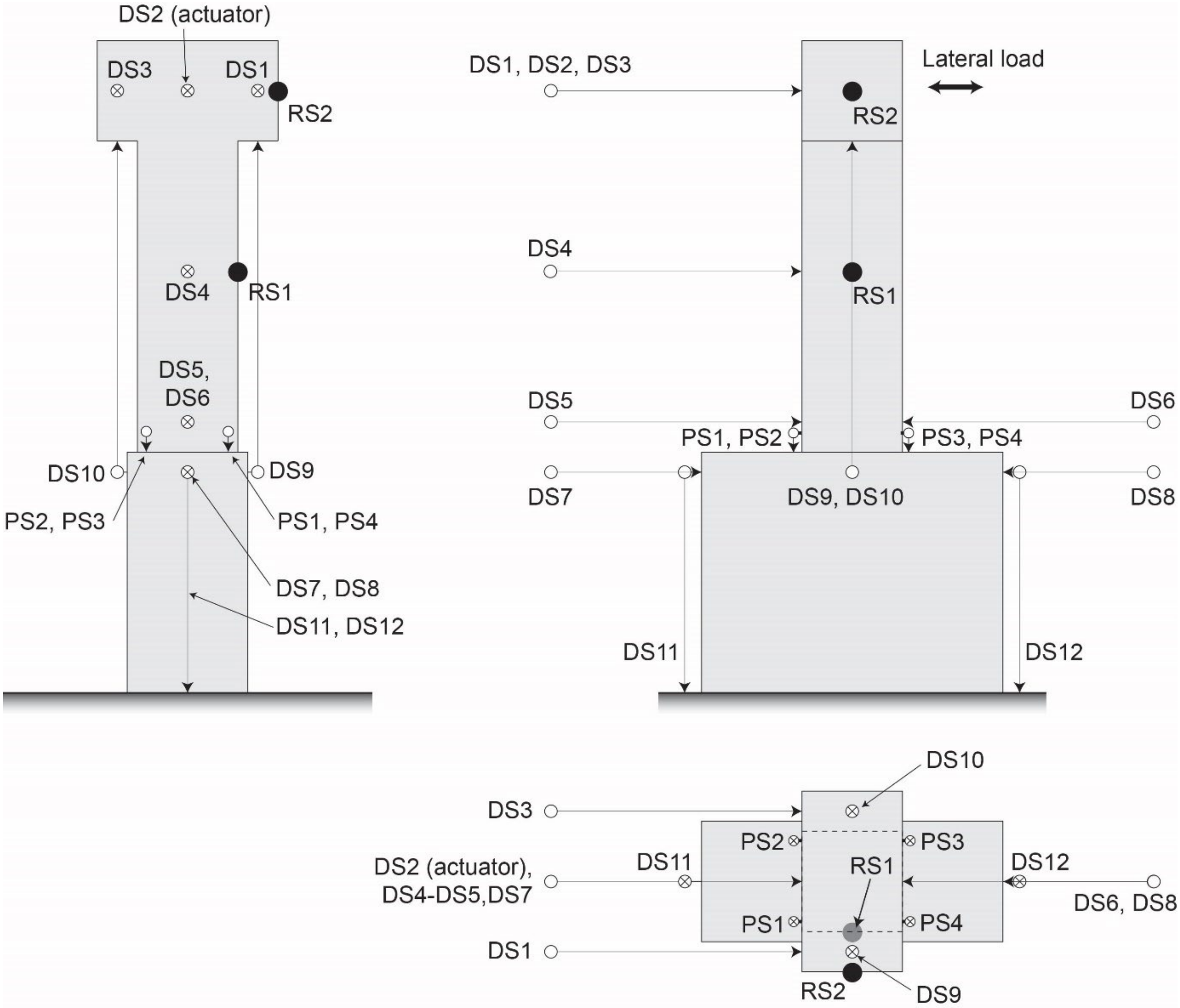

Figure 8 - Instrumentation. Note: RS = rotation sensor, DS = string potentiometer displacement sensor, PS = spring return linear position sensor.

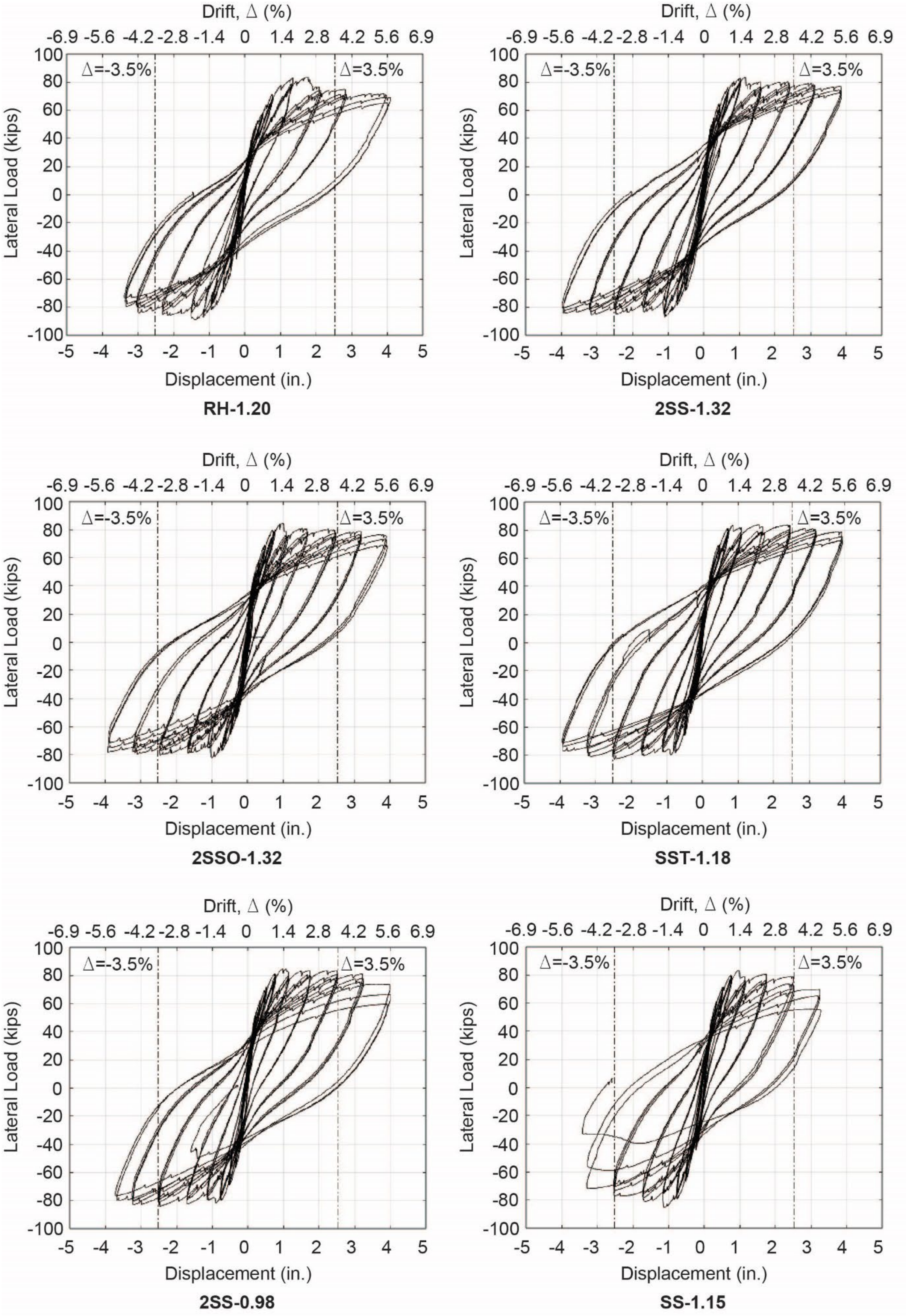

Figure 9 - Lateral load versus displacement and drift, Δ behaviors for each specimen. 1 kip = 4.45 kN; 1 in.=25.4 mm

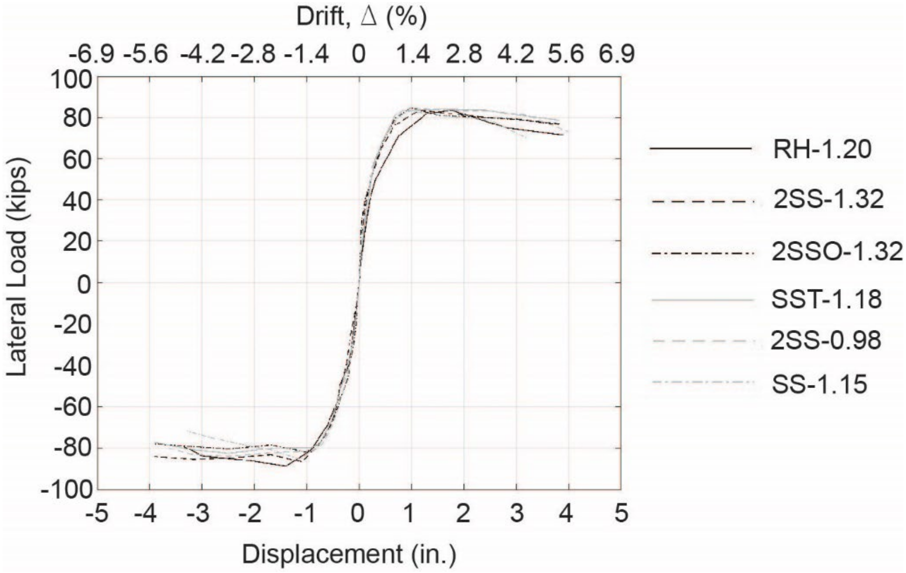

Figure 10 - Lateral load versus displacement and drift, Δ envelope for each specimen. 1 kip = 4.45 kN; 1 in.=25.4 mm

Figure 11 - Photos of excavated specimens after testing. Positive/negative indicates that compression face under that loading direction.